

MODELLING AND CONTROL OF AIRSHIP FOR LOW ALTITUDE SURVEILLANCES APPLICATION

(Date received: 08.03.12/Date accepted: 16.08.12)

Herdawatie Abdul Kadir¹ and Mohd. Rizal Arshad²

Underwater Robotics Research Group (URRG)
School of Electrical and Electronic Engineering Engineering Campus
Universiti Sains Malaysia (USM)
14300 Nibong Tebal, Pulau Pinang, Malaysia
E-mail: ¹watie@uthm.edu.my, ²rizal@eng.usm.my

ABSTRACT

Aerial perspective provide great viewing window especially for surveillance and exploration activities. In responding to the need of green technology, airship is the best alternative for environmental friendly technology. In addition, airship is safer for low altitudes flying and able to maneuver at low speed in confined area. In order to drive the airship to the desired position, the airship's rudder must generate a yaw angle. Therefore, this paper presents the techniques to control the navigation path of an airship through the yawing state response. To provide good airship heading, optimal control and feedback control technique were proposed. The main goal is to produce an appropriate output signal by controlling the rudder deflection while reducing the excessive movements of the vehicles. The simulation demonstrate that the proposed controller effectively reduced the excessive movement for yaw rate and roll angle of the airship. It is shown that closed loop system has an error less than 1.6% with minimum overshoot of 2.04%. Comparatively, better results were obtained by introducing higher gain to the optimal controller thus contribute to low control response.

Keywords: Airship, Lighter than air (LTA), LQR, Optimal control, State feedback

1.0 INTRODUCTION

Aerial surveying technique offers an attractive economic approach for large scale monitoring with larger viewing window for a scene. By introducing the cameras and sensors to the aerial surveying activities, it will provide more potential information and eventually facilitate to faster and accurate decision making. Typically, airplanes, helicopters, UAVs and balloon were used in this activity. However, this geomatics technique required a stable, low vibration and slow moving platform to acquire good information. An alternative approach is by using an airship which enables efficient solution to better aerial visibility and lower vibration effect. Moreover, it will help to monitor the area behavior over time effectively thus responds to the needs of many activities such as marine planning, climate research and accessing risk areas.

In this paper, we proposed the lighter than air (LTA) technology to perform the aerial surveying using a non rigid airship. It is a very interesting concept which enables flying with low power consumption using gas with lower densities than air to provide aerodynamic and aerostatics lift. The airship was selected for the low altitude application due to the ability to hover in longer period over a particular area. It also capable to remain stationary therefore enables many promising data to be gathered. Several research studies has carried out on airship design [1-3], lifting method [4], dynamic modeling [5-7] and application [8]. In this work, we will consider helium as the lifting gas. This monatomic gas is the second lightest element

which is very stables and nonflammables. Generally, the airships consist of 3 basic components: envelope/hull, gondola and fins as illustrated in Figure 1.

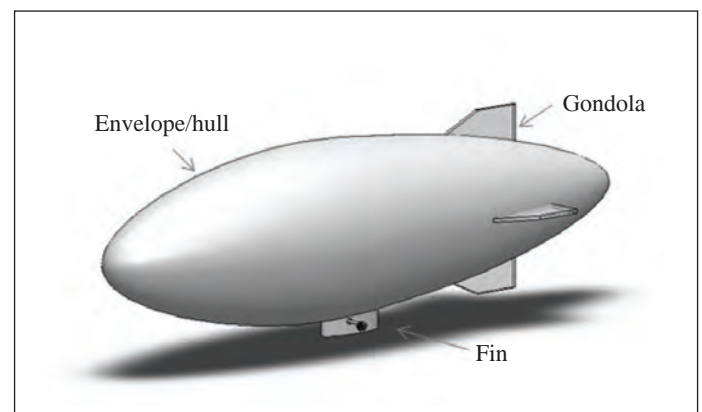


Figure 1: Airship component

The airship is able to fly slowly across a wide area for various reasons with capabilities to ascend, maneuver and descend by controlling its buoyancy. In order to obtain good information collection, the vehicles must able to follow the desired guidelines. The primary objective of this paper is to provide appropriate control signal to an airship based on the desired path. We will present two control schemes for controlling the left and right direction of the rudder deflection thus contribute to the vehicles

yawing movement. The proposed model movements were verified by introducing the control schemes. We will analyse the lateral system behavior of the airship based on the navigation path shown in Figure 2.



Figure 2: Closed loop navigation concept

The following Section II describes the dynamic model of the airship. We discuss the section by introducing assumptions, kinematics modeling and decoupled model for lateral and longitudinal. Section III present the control designs. The performances evaluation based on two controllers were presented in Section IV. Finally, Section V concludes the paper.

2.0 MATHEMATICAL MODELING

This section focuses on the formulation of integrated mathematical model of airship in state variable form. The physical dynamic effects were used to analyse the model behavior. We will briefly discuss the overall dynamics model comprises of decoupled longitudinal and lateral model [9,10].

2.1 Basic Assumptions

In order to investigate the model, it is convenient to define the references frames. There are two frames considered in this model: earth fixed references frame, F_e and body fixed references frame, F_b shown in Figure 3.

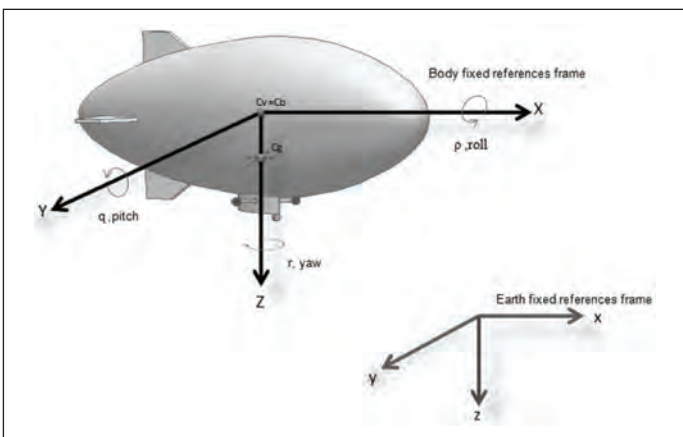


Figure 3: Two references frame. Earth References Frame (F_e) and Body Fixed Frame (F_b)

The Equation of motion (EOM) will be develop based on rigid body dynamic with several assumptions. In this case, the

origin of F_b is coincides with center of volume, C_v in the plane of symmetry. For smaller size of airship, we can assume the center of gravity, C_g lies below where the location of C_g will not change significantly. Table 1 summarizes the notation used for the airship modeling.

Table 1: Notation for blimp model

Symbol	Description	Units
u	Axial velocity perturbation	m/s
v	Lateral velocity perturbation	m/s
w	Normal velocity perturbation	m/s
p	Roll rate	rad/s
q	Pitch rate	rad/s
R	Yaw rate	rad/s
Φ	Roll attitude	Rad
θ	Pitch attitude	Rad
ψ	Yaw attitude	Rad
δr	Rudder angle	Rad
δt	Thrust angle	rad

The decoupled lateral and longitudinal model have to be postulated to describe the airship motion in flight. The earth is assumed fix and flat during the dynamic analysis. Steady flight is considered to simplify the model where small perturbation may occur [10].

2.2 Dynamic Model

The dynamic model will be discuss in two parts: Kinematics and Dynamics. The force or moment due to aerodynamics, gravitational, buoyancy, and propulsion system were incorporated in the dynamic model, which is organised into continues state-space model. The following equation decide the full nonlinear EOM written as

$$\dot{\eta} = J(\eta)v \quad (1)$$

$$M\dot{v} + fc(v)v + gb(\eta) + fd(v)v + fp = \tau \quad (2)$$

where $\eta \in \mathbb{R}^3 \times \mathbb{S}^3$ and $v \in \mathbb{R}^6$, M is the system inertia matrix, $fc(v)$ is the coriolis-centripetal matrix, $fd(v)$ is the damping matrix, $gb(\eta)$ vector of gravitational/buoyancy forces and moments, fp propulsion notation and τ is the vector of control inputs.

Kinematics: By incorporating (1) with rotation and transformation matrix. The overall 6 DOF

Equation is given by

$$\dot{\eta} = \begin{bmatrix} R^{Ob} & 0_{3 \times 3} \\ 0_{3 \times 3} & T_{\Theta} \end{bmatrix} v \quad (3)$$

where $v = [u, v, w, p, q, r]^T$ and $\eta = [x, y, z, \phi, \theta, \psi]^T$.

The model matrix, R^{Ob} denoted the rotation matrix given by

$$R^{Ob}(\Theta) = \begin{bmatrix} c\psi c\theta & s\psi c\theta + c\psi s\theta s\phi & s\psi s\theta - c\psi s\theta c\phi \\ -s\psi c\theta & c\psi c\theta - s\psi s\theta s\phi & c\psi s\theta + s\psi s\theta c\phi \\ s\theta & -c\theta s\phi & c\theta c\phi \end{bmatrix} \quad (4)$$

where $s\phi = \sin(\phi)$ and $c\phi = \cos(\phi)$ valid for $-\pi/2 < \phi < \pi/2$. While T_{Θ} is the transformation matrix simplifies to

$$T_{\Theta}(\Theta) = \begin{bmatrix} 1 & s\phi t\theta & c\phi t\theta \\ 0 & c\phi & c\psi s\phi + s\psi s\theta c\phi \\ 0 & \frac{s\phi}{c\theta} & \frac{c\phi}{c\theta} \end{bmatrix} \quad (5)$$

Dynamics: In the decoupled model, the horizontal axis and vertical axis behavior can be represent as lateral and longitudinal model. In lateral case, the state vector considered for the dynamic characteristics involve the state $x^T = [v \ p \ r \ \phi]$ and rudder deflection as the control input denoted as $u^T = [\delta_r]$. The model can be defined by the following state space representation

$$a = \begin{bmatrix} Y_v & m_z W_e & -m_x U_e & (mg - B)\cos\theta_e \\ 0 & L_p - ma_z W_e & ma_z U_e & -(mga_z - Bb_z)\cos\theta_e \\ 0 & ma_x W_e & N_r - Ma_x U_e & (mga_x - Bb_x)\cos\theta_e \\ 0 & 1 & 0 & 0 \end{bmatrix} \quad (6)$$

$$b = \begin{bmatrix} Y \\ 0 \\ \Gamma \\ 0 \end{bmatrix} \quad (7)$$

$$m = \begin{bmatrix} m_y & -ma_z & ma_x & 0 \\ -ma_z & J_x & J_{xz} & 0 \\ ma_x & -J_{xz} & J_z & 0 \\ 0 & 0 & 0 & 1 \end{bmatrix} \quad (8)$$

where $A = m/a$ is the system matrix, $B = m/b$ is the control matrix, m is the added mass matrix, J is the moment of inertia, U_e, W_e are the linear velocity component, B is the buoyancy force, b_x, b_z are the centre of volume, mg is the gravitational force, $Y, \Gamma, M_{\delta}, Z_{\delta}$ are the geometric and aerodynamic symmetry, respectively. In longitudinal model, the state vector considered for the dynamic characteristics $x^T = [u \ w \ q \ \theta]$ and $u^T = [\delta_e \ \delta_t]$

$$a = \begin{bmatrix} X_u & 0 & -m_z W_e & -(mg - B)\cos\theta_e \\ 0 & Z_w & m_x U_e & -(mg - Bb_z)\sin\theta_e \\ 0 & 0 & M_q - ma_x U_e - ma_z W_e & -(mga_x + Bb_x)\cos\theta_e + (mga_z + Bb_z)\sin\theta_e \\ 0 & 0 & 1 & 0 \end{bmatrix} \quad (9)$$

$$b = \begin{bmatrix} 0 & X_t \\ Z_{\delta} & 0 \\ M_{\delta} & 0 \\ 0 & 0 \end{bmatrix} \quad (10)$$

$$m = \begin{bmatrix} m_x & 0 & ma_z & 0 \\ 0 & m_z & -ma_x & 0 \\ ma_z & -ma_x & J_y & 0 \\ 0 & 0 & 0 & 1 \end{bmatrix} \quad (11)$$

where X_u, Z_w, M_q are the dimensional derivative symbol and derivative X_t is the trust coefficient. In order to determine the airship analysis, simulation were performed using the following features. The details are described as follows: The airship shape is consider ellipsoid with length of 1.6764 m and maximum diameter of 0.385 m. The detail of the model can found in [9].

3.0 AIRSHIP CONTROL

In order to perform the aerial surveillances, the airship should

have the ability to control the amount of rudder angles being exerted while following the desired trajectory. The control objective is to maintain the minimum control signal which takes the plant to desired states. It is practical to used decouple model of blimp while assuming small perturbation about the trimmed equilibrium [10]. In lateral control design, only the rudder will contribute to yawing with minimum roll taking place. The rudder deflection ability was set between +30 to -30 degree. In this case positive angles contribute to left deflection. The output affected by this model will be v, p, r and ϕ . Figure 5 shows the block diagram of the proposed system.

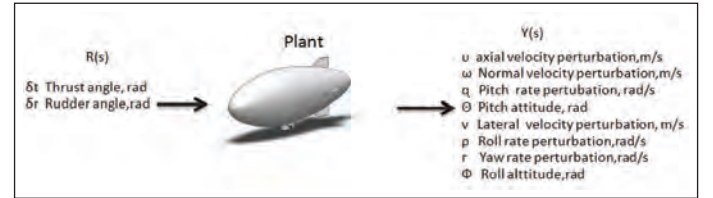


Figure 4: Lateral dynamic open loop response

An optimal control and state feedback scheme were implemented on the airship model as discusses previously. In order to study the model behavior, three initial simulations were done for designing the controller. The system model must be controllable, otherwise the control input will not affect all the states variables.

Property 1: In order to provide ability to place the pole location based our needs, is important to make sure that we obtain full rank value. The controllability matrix, C is given by $C = [B \ AB \ A^2B \ \dots \ A^{(n-1)}B]$, where B and A are representative of the EOM using state space method. Proof: Using equation (6)-(11) the forces ad moments equation based on the design proposed were written as

$$\text{Lateral model} \quad A = \begin{pmatrix} 0.0191 & 0.0175 & -5.6166 & 10.0366 \\ 0.3412 & 0.0005 & -1.0347 & 4.2577 \\ -0.0006 & 0.0000 & 0.1831 & -0.0075 \\ 0 & 1 & 0 & 0 \end{pmatrix}$$

$$B = \begin{pmatrix} 0.5131 \\ 8.9846 \\ 5.2080 \\ 0 \end{pmatrix}$$

$$\text{Longitudinal model} \quad A = \begin{pmatrix} -0.1946 & 0.0000 & -0.0114 & -9.4097 \\ -0.0009 & -0.0067 & 5.4433 & 0.1646 \\ 0.3150 & 0.0003 & -0.0376 & -0.6386 \\ 0 & 0 & 1 & 0 \end{pmatrix}$$

$$B = \begin{pmatrix} -1.2214 & 0.0189 \\ 0.9915 & 0 \\ 7.1150 & 0.0101 \\ 0 & 0 \end{pmatrix}$$

Clearly, the matrix C has full rank. The system is controllable since rank of C equal to system size of 4.

Property 2: Necessary for us to investigate what happing inside the system thus, observability O matrix, must meet the requirement given by following equation

$$\mathbb{O} = \begin{pmatrix} C \\ CA \\ \vdots \\ CA^{n-1} \end{pmatrix}$$

where C and A are representative of the EOM using state space method. *Proof:* Due to same size given, it proved that the system is observable due to full rank.

Property 3: Stability of the plant is based on eigenvalues of matrix A . For the lateral model, it contribute to these poles 2.3911, -1.2571, -1.1125 and 0.1813 and longitudinal provided 0.5746 + 1.3804i, 0.5746 - 1.3804, -1.3814, -0.0067. Since there are 2 RHP therefore the system is unstable. Figures 5 and 6 shows the simulation when an input is applied to the uncontrolled system. The decoupled models are inherently unstable, when an input is applied to the open loop system, it causes all states rise unbounded as the airship travel.

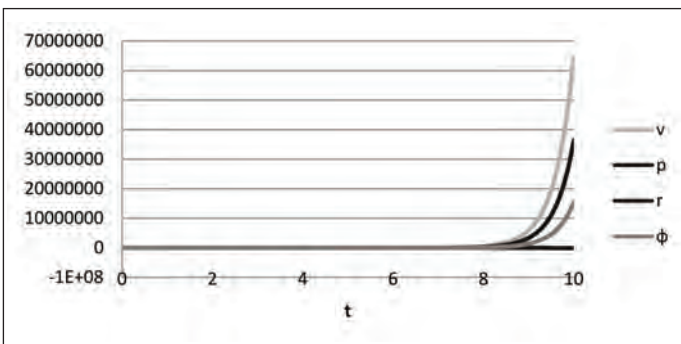


Figure 5: Lateral dynamic open loop response

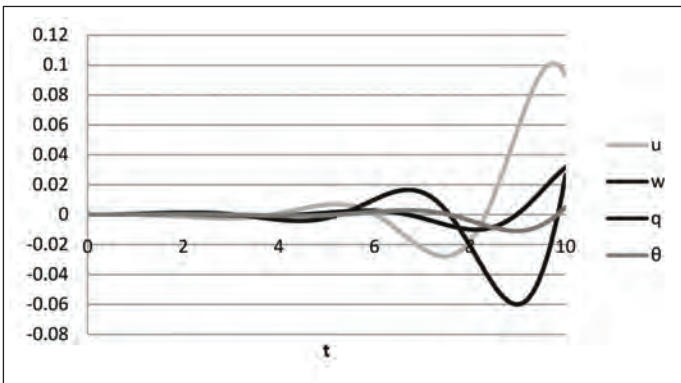


Figure 6: Longitudinal dynamic open loop response

3.1 Optimal Controller: Linear Quadratic Regulator (LQR)

The LQR method is a powerful method for designing controller for complex systems with stringent performances. This design seeks for optimal controller values that minimises control input, $u(t)$ by iterative until the desired behavior of control is achieved. The optimal value was obtained by manipulating two matrices, Q and R that weight the state vector. The performances criterion is given by

$$J(x, u) = \frac{1}{2} x^T(t_f) S x(t_f) + \int_{t_0}^{t_f} [x^T(t) Q x(t) + u^T(t) R u(t)] dt$$

where S and Q are symmetric, positive-semidefinite weighting matrices; and R is a symmetric, positive-definite weighting matrix. In this paper, the selection of Q and R metric were done based on Bryson rules. Based on the model (6) and (8), the LQR gain were given by, $K = [0.5039 \quad 3.4956 \quad -4.1256 \quad 8.3520]$.

3.2 Pole Placement by State Feedback Controller

In this control scheme, the designer able relocates all the closed loop poles of the system to desired locations. The selections of values of the state feedback vector effect the shape of the plant output. In order to meet the design specification, the best value of poles and zeros becomes a matter of trial and error. The poles of the system have to be placed carefully due to costs that are associated with shifting pole locations. For best results, several simulation trials using MATLAB have to be performed to achieve desired response while not straining the control input, $u(t)$. According to a control law as follows

$$u(t) = K[x_d(t) - x(t)]$$

where $x(t)$ is the state-vector of airship, $x_d(t)$ is the desired state-vector. The controller aims to achieve desired rudder deflection if the airship model in the steady state. The input vector, $u(t)$ were used as input to model. The final results of tuning for the optimal pole location to achieve desired objectives are $P = [-1, -2, -2.89, -3]$. These values contribute to controller gain $K = [0.4574, 3.2026, -3.8241 \text{ and } 7.5774]$.

4.0 RESULTS

In this section, we present two continuous-time based controllers: The optimal controller (LQR) and state feedback controller using pole placement method with reference input. The design of controller is based on the lateral modeling for driving the airship to monitoring an area. The navigation path was given based on the scene to be view. In this work, the navigation path was set as shown in Figure 7. For desired input, the peak value were 0.0172 rad which contribute to 1 degree, with each pulse stay for 8s (enough time to converge to steady state) and assuming time taken to monitor small area is 80 second.

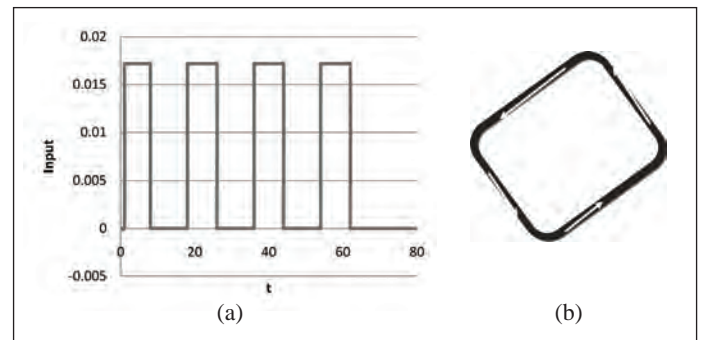


Figure 7: Desired input for rudder deflection (a) signal generated based on anticlockwise looping (b) proposed navigation

4.1 Linear Quadratic Regulator (LQR)

Referring to Section III, we have implemented the proposed control scheme on our model. The summarises result obtained from the simulation are given in Table III. The input unit was described in degree to represent the real behavior of the blimp. Figure 8 illustrated the overall lateral states behavior when 1

degree of deflection is applied. The simulations were done using Matlab/Simulink software. The control Q and R matrix follows the Bryson rules by introducing gain value of 1 in the selected matrix area to show that the model adaptability. The result shows, that the control unit, $u(t)$ value are able to stabilise the airship within approximately -0.016 to 0.016 , it is rather small thus minimises the controlling cost.

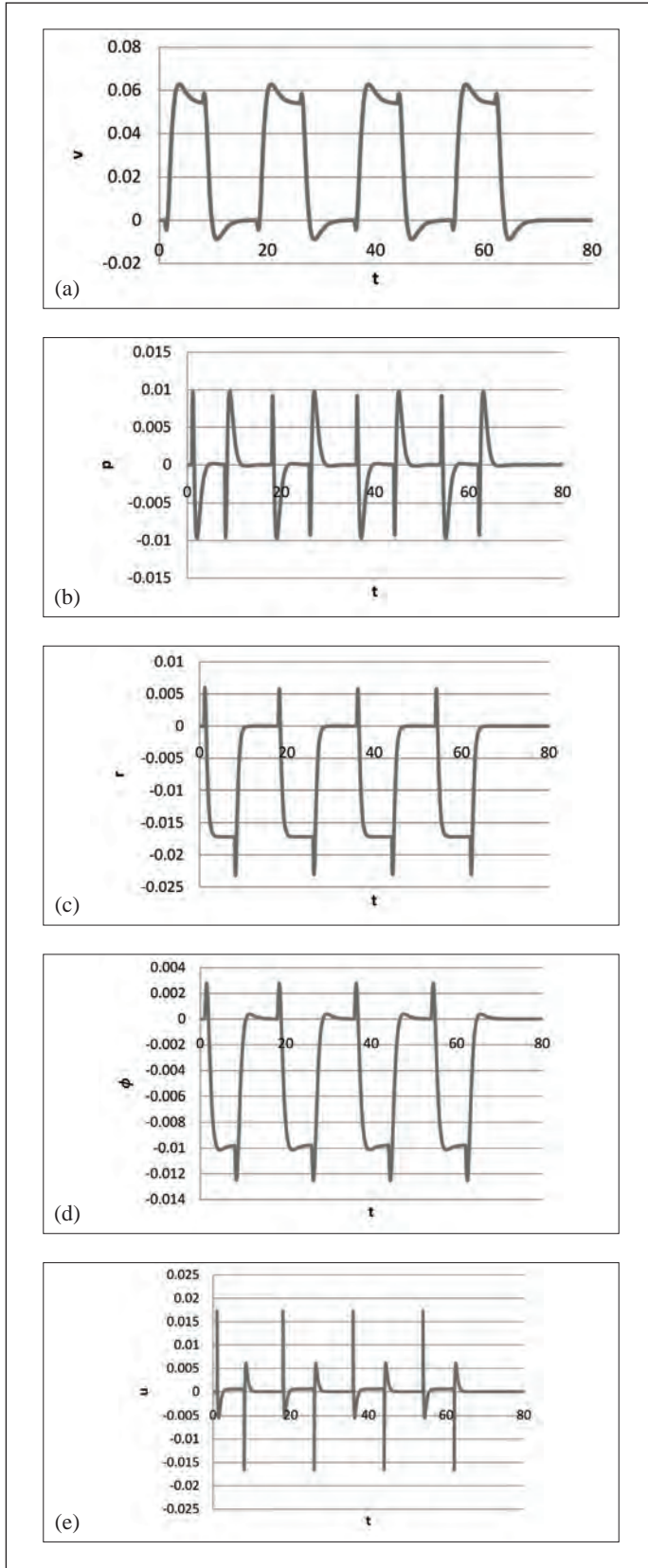


Figure 8: Output for rudder deflection for overall states (a) velocity (b) roll rate (c) yaw rate (d) roll altitude (e) control unit

Using desired input value 1 deg (0.0172 rad), the airship should be able to yaw to the left. Note that positive angles contribute to left deflection on the yawing angles. Figure 9 show that the positive angles contribute to negative angles reflecting the negative values as the left deflection. This proves the model behavior follow the design requirement. In order to observe the behavior of vehicles navigation, a range of input were given between 0 and 30 degree. The opposite values give similar amplitude value but with different polarity.

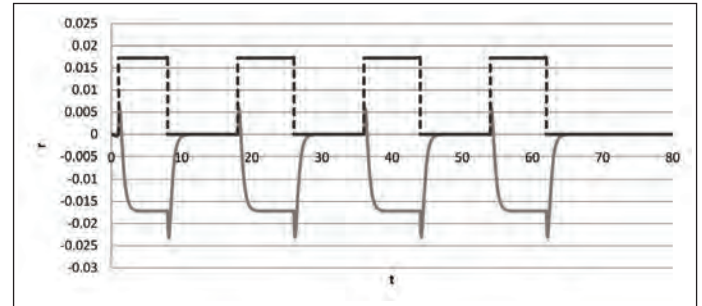


Figure 9: Output versus actual, r

In this analysis, a pulse was injected for 8 second for 4 times to sample the behavior of closed loop navigation. If longer pulse were given the same shape of response will be display but with different time range. However if small time pulse were given the system will not have enough time to stables the previous cycles signal and continuing to overcome new goal.

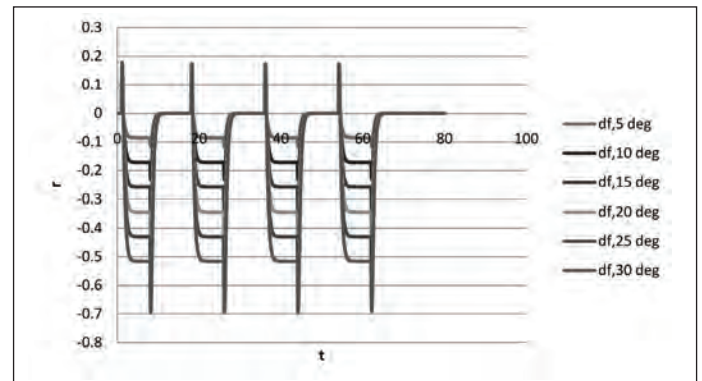


Figure 10: Actual output of rudder deflection

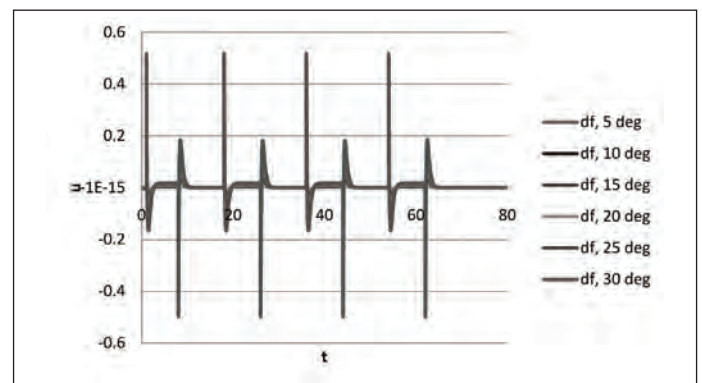


Figure 11: Control signal, $u(t)$ of LQR

Rudder angles simulation

The dynamic is input with angle of 0 to 30 degree using input as shown in Figure 7. The smaller time values were used as samples to analyses the system behavior. The responses of the states were shown in Figure 10. Note that this based on 180 degree left and

right movement. The system responses for yaw rate for each deflection concluded in Table 2 and 3. All results were describes in degree unit.

Table 2: Result of the simulations

	Time, s	5 deg	10 deg	15 deg	20 deg	25 deg	30 deg
Rise time, Tr	2.4151	-4.31	-8.63	-12.95	-17.27	-21.58	-25.89
Peak time, Tp	1.1458	1.71	3.41	5.12	6.83	8.54	10.24
OS%	Nil	Nil	Nil	Nil	Nil	Nil	Nil
Settling time, Ts	-4.9617	-4.92	-9.84	-14.77	-19.69	-24.61	-29.53
min point	8.1732	-6.65	-13.29	-19.93	-26.57	-33.22	-39.86

Table 3: Result of the simulations

Desired	Actual	e	e %
5	4.9224	0.0776	1.5525
10	9.8447	0.1553	1.5525
15	14.7671	0.2329	1.5525
20	19.6895	0.3105	1.5525
25	24.6119	0.3881	1.5525
30	29.5342	0.4658	1.5525

Table 2 describes the output responses characteristic for each deflection. The results shows that each rudder deflection follows the target value quickly without overshoot. The proposed LQR output gives good results however each transition suffer from inverse movement in short time. This reflect to the real effect of the vehicle that may affected by sliding issues. In Table 3, the desired and the actual value are listed for vehicles yawing. It can be concluded that the error contribute approximately 1.6 % with control unit amplitude of max deg of ± 0.516 and min deg of ± 0.086 . The results confirm the design able to accomplish the control objective.

4.2 Pole Placement by State Feedback Controller

Next, by repeating the same model analysis with statefeedback controller. Results for this scheme are shown in Figure 12. The summarises result were presented in Table 6 and 7. In this control technique, we placed the desired poles on the left half plane of s-plane for stability. The values of K are obtained by introducing several poles during the simulation based on the trial and error concept.

By introducing 1 deg (0.0172 rad) of input to the model, all states are able converge to target response. Figure 12 shows, the positive angles deflection of rudder contribute to left deflection on the yawing angles. The system responses for yaw rate for each deflection were concluded in Table 4 and 5.

The results shows that the system able to achieve desired output although with overshoot. From the observation the similar output shape response obtained from previous scheme. In Table 3, the desired and the actual value are listed for vehicles yawing. It can be concluded that the error contribute approximately 0.7 % smaller than LQR result.

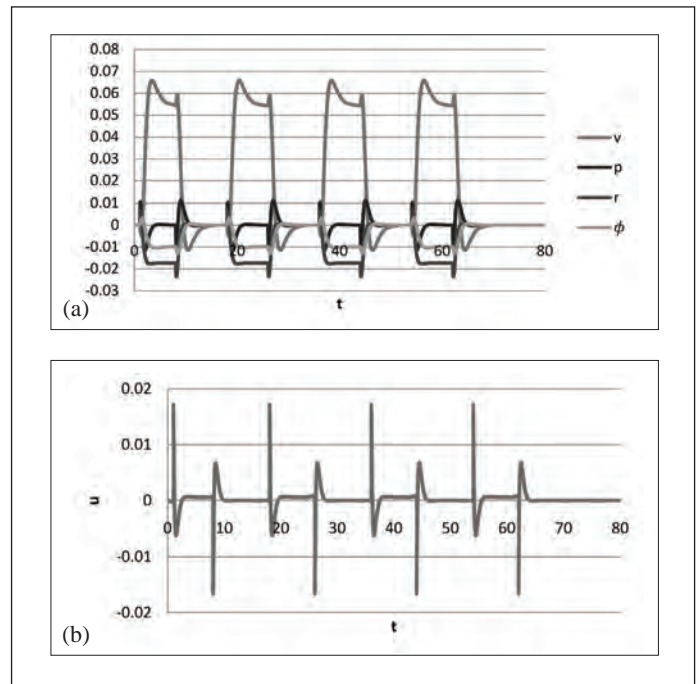


Figure 12: State feedback system design (a) States response output using state feedback (b) Control signal, u(t)

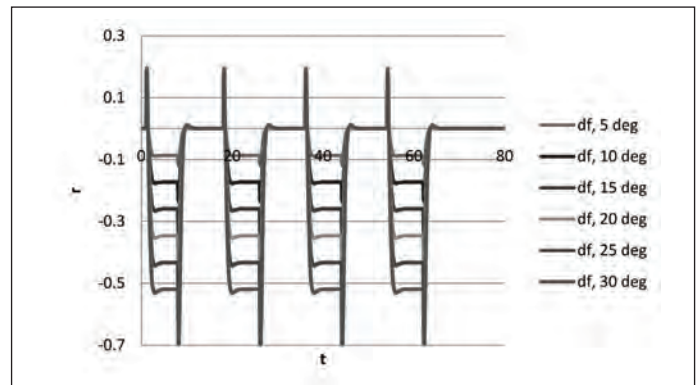


Figure 13: Actual output of rudder deflection

Table 4: Result of the simulations

	Time, s	5 deg	10 deg	15 deg	20 deg	25 deg	30 deg
Tr	2.438646	-4.851	-9.702	-14.552	-19.403	-24.254	-29.105
Tp	1.156074	1.864	3.727	5.591	7.454	9.318	11.181
OS	2.837457	-0.101	-0.202	-0.304	-0.404	-0.506	-0.607
Ts	6.7601	-4.961	-9.922	-14.884	-19.845	-24.806	-29.766
Min point	8.128674	-6.742	-13.484	-20.226	-26.967	-33.710	-40.451

Table 5: Result of the simulations

Desired	Actual	e	e %
5	4.9611	0.0389	0.7776
10	9.9222	0.0778	0.7776
15	14.8834	0.1166	0.7776
20	19.8445	0.1555	0.7776
25	24.8056	0.1944	0.7776
30	29.7667	0.2333	0.7776

The results of both controllers were compare to validate the achievement of each parameter. The responses on each states difference were illustrated in Figure 14 and 15. We see that small different occur for each state. The LQR and state feedback have similar response shape. LQR able to minimize the control cost without overshoot and complete the cycle quickly. However recorded higher error than the state feedback controller. Even though the state feedback gives better result in term of error, rise time and settling time. The system comes with 2% of overshoot for each desired deflection.

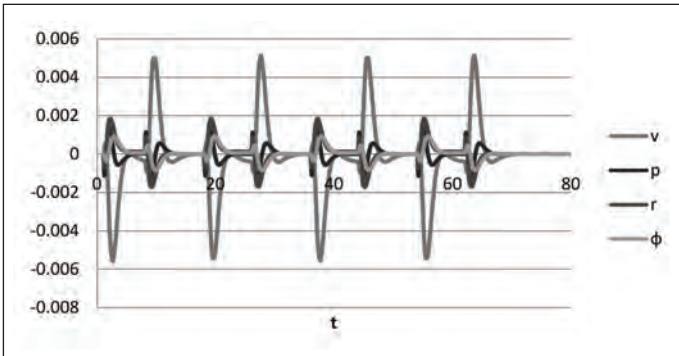


Figure 14: Output response difference between two controller

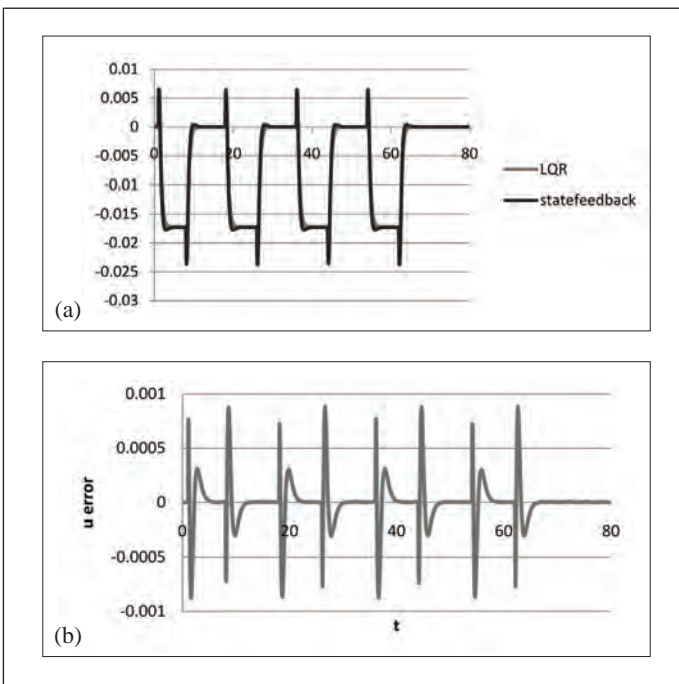


Figure 15: Comparisons (a) Comparison of yaw rate
(b) Error difference between two controllers

For $|e|$, LQR has higher value of 1.6% than state feedback 0.78 %. In this design the LQR, the matrix value was based on Bryson rule without increasing the gain. In order to achieve better result higher value of Q matrix can be introduce to improve the system behavior. The details of each parameter are shown in Table VI and VII.

Throughout the analysis, both controllers are able to achieves the control objectives. Although LQR method contributes to higher error compare to the state feedback, this method is more robust. Therefore only a small different occur between these two controller with very small error for yawing rate thus contribute to good navigation results.

Table 6: Controller comparison

(SS-LQR)	Time, s	5 deg	10 deg	15 deg	20 deg	25 deg	30 deg
Tr	0.023546	-0.54	-1.07	-1.61	-2.14	-2.67	-3.20
Tp	0.010274	0.16	0.31	0.47	0.62	0.78	0.93
OS	2.837457	-0.10	-0.20	-0.30	-0.40	-0.51	-0.61
Ts	1.7984	-0.04	-0.08	-0.11	-0.15	-0.19	-0.23
Min point	-0.04453	-0.10	-0.20	-0.30	-0.40	-0.49	-0.60

Table 7: Controller comparison

Desired	Actual	e	e %
5	0.0387	0.0387	0.7749
10	0.0775	0.0775	0.7749
15	0.1163	0.1163	0.7749
20	0.155	0.155	0.7749
25	0.1937	0.1937	0.7749
30	0.2325	0.2325	0.7749

5.0 CONCLUSION

In this paper, an airship model that will be used in navigation is analysed. The small airship modeling is based on our design requirement. The configuration of an airship will affect the model controllability and the control law response. Two lateral lateral controllers we proposed in Section III enable the rudder deflection control that define the yawing rate and roll of the airship. Although, our model was unstable, the proposed controllers were able to help the airship achieve navigation path. However, these methods need to be tune several times in order to obtain the best states response. We have proven that both controller, were sufficient for the airship to reach the goal. For more robust application, the LQR gives more effectives control strategies thus offer precise control for airship heading with less tuning.

ACKNOWLEDGEMENT

The authors would like to thank Malaysia Ministry of Science, Technology and Innovation (MOSTI), e-Science 305/PELECT/6013410, Ministry of Higher Education (MOHE), Universiti Sains Malaysia and Universiti Tun Hussein Onn Malaysia for supporting the research. They would also like to thank Khalid Isa and anonymous reviewers for their comments and suggestion. ■

REFERENCES

- [1] P. González, W. Burgard, R. Sanz, and J.L. Fernández, "Developing a Low-Cost Autonomous Indoor Blimp" *Journal of Physical Agents*, vol. 3, pp. 43-51, 2009.
- [2] Y. Li, M. Nahon, and I. Sharf, "Airship dynamics modeling: A literature review," *Progress in Aerospace Sciences*, vol. 47, pp. 217-239, 2011.
- [3] G. Liu, F. Wang, and G. Hong, "Dynamic modeling and dynamic characteristic analysis of a new concept stratospheric V-shaped airship," vol. 145, pp. 37-42, 2012.

- [4] W. Xiao-liang, M. Ye, and S. Xue-xiong, "Modeling of stratosphere airship," in *International Symposium on Systems and Control in Aeronautics and Astronautics (ISSCAA)*, pp. 738-743. 2010.
- [5] S. Bennaceur and N. Azouz, "Contribution of the added masses in the dynamic modelling of flexible airships," *Nonlinear Dynamics*, vol. 67, pp. 215-226, 2012.
- [6] E. Hygounenc, I.-K. Jung, P. Souères, and S. Lacroix, "The autonomous blimp project of laas-cnrs: Achievements in flight control and terrain mapping," *International Journal of Robotics Research*, vol. 23, pp. 473-511, 2004.
- [7] E. J. Brandreth, Jr., "Airships: an ideal platform for human or remote sensing in the marine environment," *Conference and Exhibition in OCEANS*, vol 3, pp. 1883-1885, 2000.
- [8] P. Luca, O. Per, and G. Christopher, "Micro- and Nano-Air Vehicles: State of the Art," *International Journal of Aerospace Engineering*, Hindawi Publishing Corporation, 2011.
- [9] Herdawatie Abdul Kadir, M.R. Arshad and Husaini A.B "Modeling and Control analysis of URRG Monohull Blimp" in *Proceedings of the International Symposium on Robotics & Intelligent Sensors*, 2012 (accepted).
- [10] G.A. Khoury and J.D. Gillet, *Airship Technology*: Cambridge University Press, United Kingdom, 1999.
- [11] T.I. Fossen, *Marine Control Systems: Guidance, Navigation and Control of Ships, Rigs and Underwater Vehicles*, Marine Cybernetics: Trondheim, Norway, 2002.
- [12] J.R. Raol and J. Singh, *Flight mechanics modeling and analysis*, Boca Raton: FL: CRC Press, 2009.

PROFILES



ENGR. ASSOCIATE PROFESSOR DR MOHD. RIZAL ARSHAD graduated from University of Liverpool, in 1994 with a B.Eng. In Medical Electronics and Instrumentation. He then pursued his MSc. in Electronic Control Engineering at the University of Salford, graduating in December 1995. Following from this, in early 1999, he completed his PhD degree in Electrical Engineering, with specialisation in robotic vision system. He is currently an Associate Professor and the deputy dean of the School of Electrical and Electronic Engineering, Universiti Sains Malaysia and with his team of researcher, is also the pioneer of underwater system technology research efforts in Malaysia, known as URRG. His is very interested in investigating the fusion of the natural world with the modern engineering pool of knowledge. This is the reason his group has embarked on the bio-inspired research efforts and the utilisation of nature to complement the current robotics system.



MS. HERDAWATIE ABDUL KADIR received the Bachelor degree in electrical and electronics engineering from Universiti Teknologi Malaysia in 2001 and the master degree in mechatronic and automatic control in 2005. She is currently working toward the PhD degree in computational intelligence at URRG, University Sains Malaysia. Her current research interest include modeling, control, localisation and Mapping.